Exploiting Input Cyclostationarity for Blind Channel Identification in OFDM Systems

Robert W. Heath, Jr. and Georgios B. Giannakis

***Abstract*— Transmitter-induced cyclostationarity has been explored recently as an alternative to fractional sampling and antenna array methods for blind identification of FIR communication channels. An interesting application of these ideas is in OFDM systems, which induce cyclostationarity due to the cyclic prefix. In this correspondence, we develop a novel subspace approach for blind channel identification using cyclic correlations at the OFDM receiver. Even channels with equispaced unit circle zeros are identifiable in the presence of any nonzero length cyclic prefix with adequate block length. Simulations of the proposed channel estimator along with its performance in OFDM systems combined with impulse response shortening and Reed–Solomon coding are presented.**

I. Introduction

Recently, there has been interest in filter bank precoding for communication systems impaired by frequency-selective fading channels [5], [14]. Although similar forms of precoding have been considered in the past [7], current interest focuses on the introduction of discrete-time cyclostationarity by the multirate precoder to enable blind channel identification at the receiver. Transmitter-induced cyclostationarity, which can be introduced either with filter banks [5], repetition coding [14], or modulation [13], allows for blind identification of arbitrary FIR multipath channels without zero-restrictions as in blind fractional sampling methods [4]. One application of transmitter-induced cyclostationarity for blind channel identification is orthogonal frequency division multiplexing (OFDM) systems that can be considered a special case of the precoding structure presented in [5].

OFDM has found renewed interest in recent years due to applications such as digital terrestrial TV [12], indoor wireless networks [2], and mobile communications [11], which are all systems that require communication in severe multipath channels. By inserting a cyclic prefix before each transmitted block longer than the order of the channel, OFDM effectively turns a frequency-selective channel into a flat-fading channel. This allows, for simple, one-tap vector equalization at the expense of a loss of 10–25% in efficiency due to the extra symbols required by the cyclic prefix [17] as well as increased sensitivity to timing, frequency synchronization [15], and transmission nonlinearities accentuated by the nonconstant modulus of OFDM signals. Channel estimation in these systems is performed by inserting training data in either the time or the frequency domain, further decreasing the efficiency. Alternatively, differential encoding may be used in place of equalization if a constant modulus constellation (say, QPSK) is transmitted at the expense of less bandwidth efficiency. Unfortunately, if the channel impulse response is longer than the cyclic prefix, interference occurs, and the simple equalization property is lost.

Manuscript received August 14, 1997; revised June 23, 1998. This work was supprted by the Office of Naval Research under Grant N00014-95-1-0908. The associate editor coordinating the review of this paper and approving it for publication was Prof. James A. Bucklew.

R. W. Heath, Jr. is with the Information Systems Laboratory, Stanford University, Stanford, CA 94305-9510 USA (e-mail: rheath@stanford.edu).

G. B. Giannakis was with the Department of Electrical Engineering, University of Virginia, Charlottesville, VA 22903-2442 USA. He is now with the Department of Electrical Engineering, University of Minnesota, Minneapolis, MN 55455 USA.

Publisher Item Identifier S 1053-587X(99)01348-3.

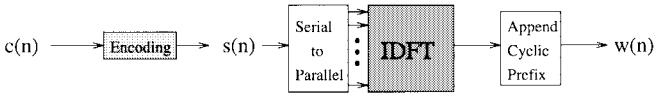

Fig. 1. OFDM transmitter.

In this correspondence, we use the cyclostationarity induced by the cyclic prefix in the OFDM system to develop an algorithm for blind channel estimation. The subspace approach of [13] is generalized here to multirate precoders and is proposed for OFDM systems as an alternative to the nonlinear matching approach of [5]. The blind nature of this estimation allows more data to be used for information transfer or for coding. As shown in [6], this approach is robust to the presence of stationary noise and channel overestimation error and does not require the cyclic prefix to be longer than the channel memory. Since we can estimate channels regardless of the cyclic prefix and without training data, the conclusion in [17] that channel coding is better than subchannel equalization must be re-evaluated. A blind algorithm for equalization was considered in [3], which uses a property of the digital-to-analog converter at the receiver and does not employ a cyclic prefix. With the absence of a cyclic prefix, however, this approach can only result in partial elimination of the intersymbol interference caused by the channel.

This correspondence is organized as follows. In the next section, we provide an overview of the OFDM system. Section III then considers the problem of blind channel identification using the cyclostationarity inherit in the OFDM transmitter. We present simulations of the proposed algorithms in Section IV.

II. The OFDM System

Consider the OFDM transmitter in Fig. 1. The OFDM modulator takes the M-point IDFT of a block of M input symbols from the coder and appends a sequence of $L < M$ symbols to the beginning of each block (see Fig. 2). In this way, the OFDM modulator can be viewed as a rate $M/(M+L)$ block code operating in the real field. To describe the input/output relationship at various points, let $P = M + L$, and adopt the polyphase notations $s_m(n) = s(nM+m)$, $w_p(n) = w(nP+p)$, $x_p(n) = x(nP+p)$ to denote the mth or pth symbol in the nth block of data at the input to the modulator, output of the modulator, and at the output of the channel, respectively (see Figs. 1–3). Then, the sequence to be transmitted is

$$w_p(n) = \sum_{m=0}^{M-1} s_m(n) e^{j\frac{2\pi}{M}m(p-L)}, \quad p = 0, \ldots, P-1 \qquad (1)$$

with the $\exp(j2\pi m(-L)/M)$ accounting for the cyclic prefix, which is a repetition of the last L frequency domain symbols as in Fig. 4. During transmission, $w_p(n)$ is pulse-shaped with $g_c^{(\mathrm{tr})}(t)$, propagates through an unknown frequency selective channel $g_c^{(\mathrm{ch})}(t)$, is degraded by additive white Gaussian noise (AWGN) $\nu_c(t)$, and is filtered by $g_c^{(\mathrm{rec})}(t)$ on reception. With $\star$ denoting linear convolution, let $g_c(t) = g_c^{(\mathrm{tr})}(t) \star g_c^{(\mathrm{ch})}(t) \star g_c^{(\mathrm{rec})}(t)$ and $h(n) = g_c(nT+\epsilon)$ denote the order L_h composite discrete-time channel, and let $v(n) = g_c^{(\mathrm{rec})}(t) \star \nu_c(t)|_{t=nT+\epsilon}$ denote the received AWGN (assuming Nyquist pulse shaping). Note that the channel model explicitly incorporates the symbol timing error $\epsilon \in [0, T)$. Assuming that the block size

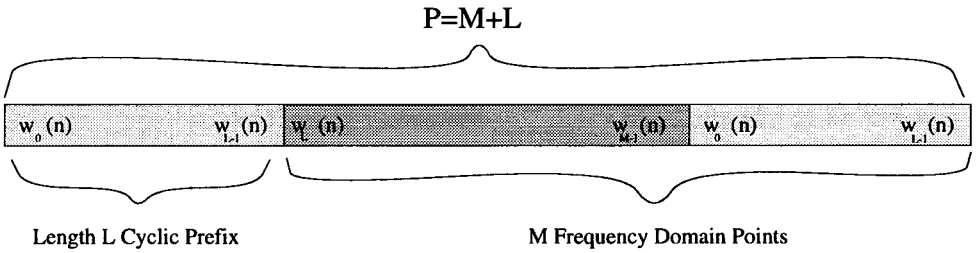

Fig. 2. OFDM frame structure.

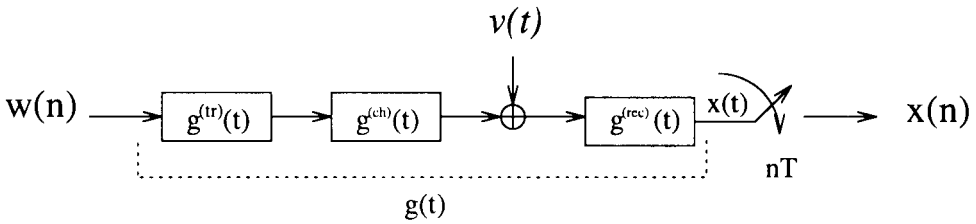

Fig. 3. Baseband equivalent transmission channel.

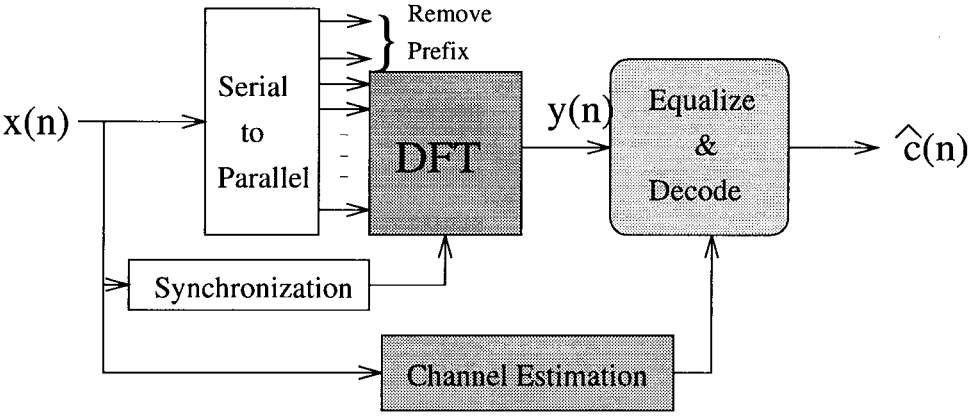

Fig. 4. OFDM receiver.

M is greater than L_h, only two blocks can overlap due to ISI. We use polyphase notation to separate the channel output $x(n) = \sum_{l=0}^{L_h} h(l)w(n-l) + v(n)$ into one part that depends on the present symbols $s_m(n)$ and one part that depends on the past symbols $s_m(n-1), m \in [0, M-1]$. Then, the input to the OFDM demodulator for $p \in [0, P-1]$ is

$$x_p(n) = \sum_{m=0}^{M-1} s_m(n) e^{j\frac{2\pi}{M}m(p-L)} \sum_{l=0}^{L_h} h(l) e^{-j\frac{2\pi}{M}ml} \times \sum_{r=0}^{P-1} \delta(r-(p-l)) + \sum_{m=0}^{M-1} s_m(n-1) e^{j\frac{2\pi}{M}m(p-L)} \times \sum_{l=0}^{L_h} h(l) e^{-j2\pi m(l-P)} \delta(r-(p-l+P)) + v_p(n) \quad (2)$$

where the summation over deltas constrains the ranges of $(p-l)$ and $(p-l+P)$ to lie in $[0, P-1]$. Assuming correction for frequency offset [15], the demodulator then removes the first L symbols corresponding to the cyclic prefix and takes the M-point DFT to obtain $y_k(n) = \frac{1}{M}\sum_{p=0}^{M-1} x_{p+L}(n) e^{-j\frac{2\pi}{M}pk}$, which, in general, equals

$$y_k(n) = \frac{1}{M} \sum_{m=0}^{M-1} s_m(n) \sum_{p=0}^{M-1} e^{j\frac{2\pi}{M}p(m-k)} \sum_{l=0}^{L_h} h(l) e^{-j\frac{2\pi}{M}ml} \times \sum_{r=0}^{P-1} \delta(r-(p+L-l)) = \frac{1}{M} \sum_{m=0}^{M-1} s_m(n-1) \sum_{p=0}^{M-1} e^{j\frac{2\pi}{M}p(m-k)} \sum_{l=0}^{L_h} h(l) e^{-j\frac{2\pi}{M}m(l-P)} \times \sum_{r=0}^{P-1} \delta(r-(p+L-l+P)) + v_k(n) \quad (3)$$

where $v_k(n)$ is the transformed noise. By choosing the cyclic prefix to be as long as the order of the channel, e.g., $L \geq L_h$, the second sum in (3) becomes zero because $(p-l+L+p) \in [P, 2P+L_h-1] \notin [0, P-1]$. The sum over p in the first term becomes $\delta(m-k)$ since $(p-l+L) \in [0, P-1]$, and thus, (3) simplifies to (in the absence of noise)

$$y_k(n) = s_k(n) H\left(\frac{2\pi}{M}k\right). \quad (4)$$

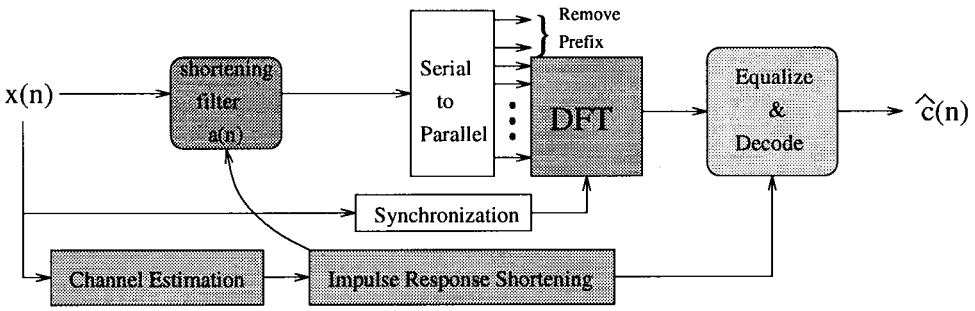

Fig. 5. OFDM receiver with impulse response shortening.

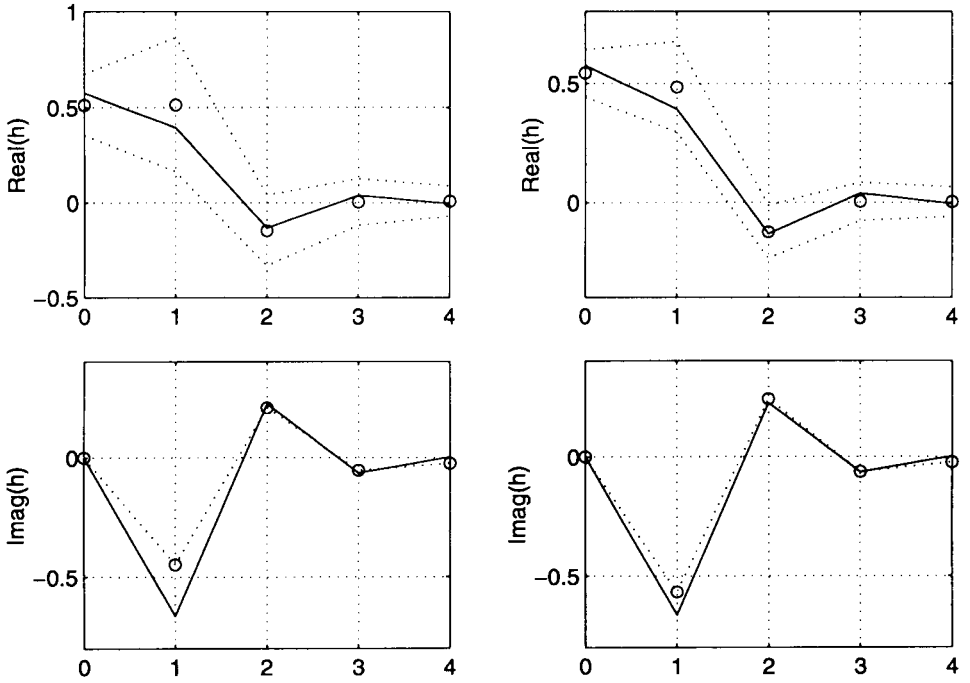

Fig. 6. Averaged channel estimates ± standard deviation for $P = 19$, $M = 15$, $I = 100$, and SNR $= 20$ dB.

The fact that OFDM effectively turns a frequency-selective fading channel into a flat-frequency fading channel is evident in (4). Clearly, equalization amounts to correcting $y_k(n)$ for a phase and a scale factor for each k. In fact, for PSK constellations incorporated with subchannel differential encoding, channel estimation is unnecessary. Unfortunately, many applications use nonconstant modulus symbol sets to improve transmission efficiency, thus requiring the estimation of $\{H(2\pi k/M)\}_{k=0}^{M-1}$.

The ease in equalization due to (4) is not without drawbacks. The presence of the DFT at the receiver places stricter requirements on synchronization [15]. Additionally, (4) exhibits reduced performance in spectral nulls. In wireline transmission schemes such as discrete multitone transmission (DMT), the channel knowledge is used by the transmitter for adaptive loading and/or power control [1]. In broadcast and wireless OFDM, this problem is resolved by using coding. A variety of schemes for coding have been proposed, typically employing some sort of convolutional coding, interleaving, and concatenation [8], for the purpose of correcting the resulting bursty errors.

Since the length of the cyclic prefix is chosen *a priori*, interference occurs as shown in (3) due to the coefficients of $h(l)$, for $l > L$. This creates problems in channel estimation that relies on the structure in (4) and results in symbol errors caused by the ISI term. This problem can be eliminated by employing decision feedback [16] or impulse response shortening [9]. Since decision feedback has a complexity that increases with the size of the DFT, we focus on impulse response shortening (see Fig. 5), which consists of designing a prefilter $a(n)$ such that the composite channel $a(n) \star h(n)$ has energy concentrated in the desired duration chosen for the cyclic prefix [9]. In the next section, we develop an algorithm for blind channel estimation that does not require the channel to be shorter than the cyclic prefix. We apply impulse response shortening when the channel duration exceeds the duration of the cyclic prefix. This approach allows for a reduction of the cyclic prefix and elimination of training data so that the system can provide a higher data rate or greater reliability through increased coding.

III. Blind Channel Identification

With the presence of a cyclic prefix in the OFDM transmission scheme, we are motivated to look for cyclostationarity in the output of the encoder as in [5]. Assume the symbols $s_m(n)$ from the encoder in Fig. 1 are white and zero-mean with variance σ_s^2, take $P > M$, and,

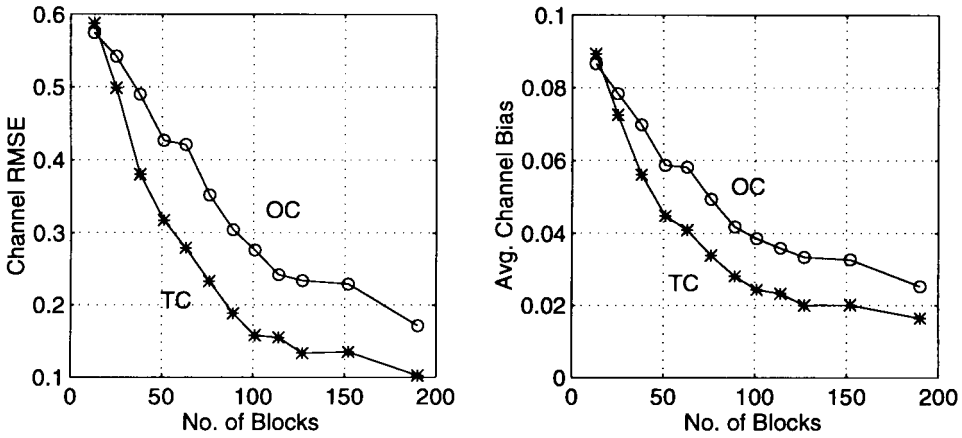

Fig. 7. Channel error versus number of symbols for $M = 15$, $P = 19$, $I = 100$, SNR $= 20$ dB.

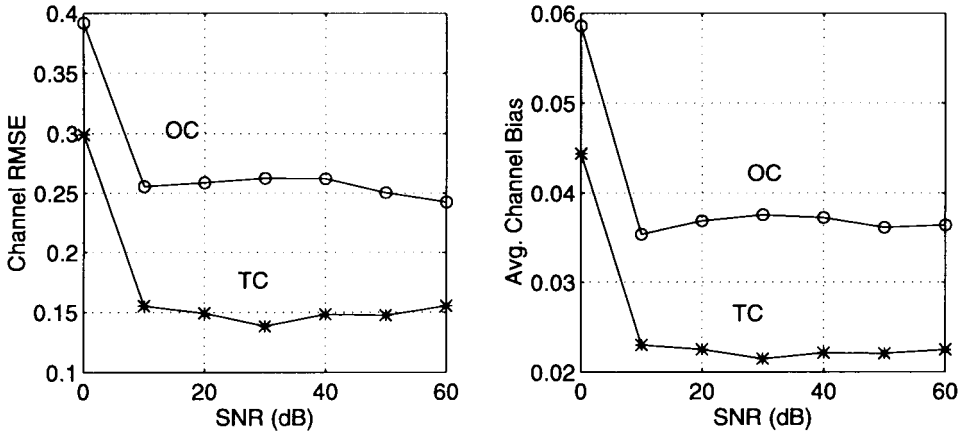

Fig. 8. Channel error versus SNR for $M = 15$, $P = 19$, $I = 100\,120$ M data.

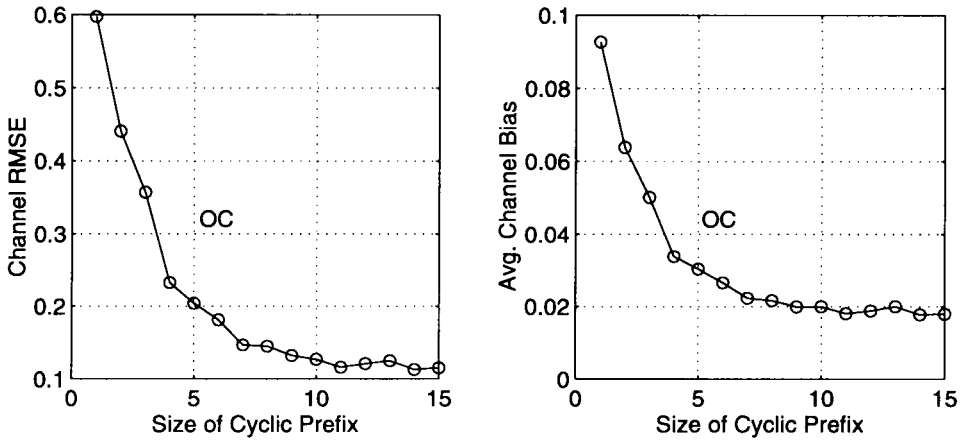

Fig. 9. Channel error versus size of cyclic prefix for $M = 15$, $I = 100\,120$ M data (with $P = M + L_h$ varying accordingly).

using (1), examine the time-varying correlation $c_{ww}(nP + p; \tau) := E\{w_p(n)w^*_{p+\tau}(n)\}$ at the output of the modulator

$$c_{ww}(nP+p;\tau) = \sum_{m_1=0}^{M-1}\sum_{m_2=0}^{M-1} E\left\{s_{m_1}(n)s^*_{m_2}(n)\right\} e^{j\frac{2\pi}{M}m_1(p-L)} \times e^{-j\frac{2\pi}{M}m_2(\tau+p-L)} \sum_{r=0}^{P-1}\delta(r-(p+\tau)) \quad (5)$$

$$= \sigma_s^2 M\left[\delta(\tau)+\delta(\tau-M)\sum_{r=0}^{P-M-1}\delta(p-r) + \delta(\tau+M)\sum_{r=M}^{P-1}\delta(p-r)\right]. \quad (6)$$

Since the right-hand side of (6) depends only on p, the output of the encoder is cyclostationary with period P. Note that if we take $P = M$, then (6) would instead become $c_{ww}(nP+p;\tau) = \sigma_s^2 M\delta(\tau)$

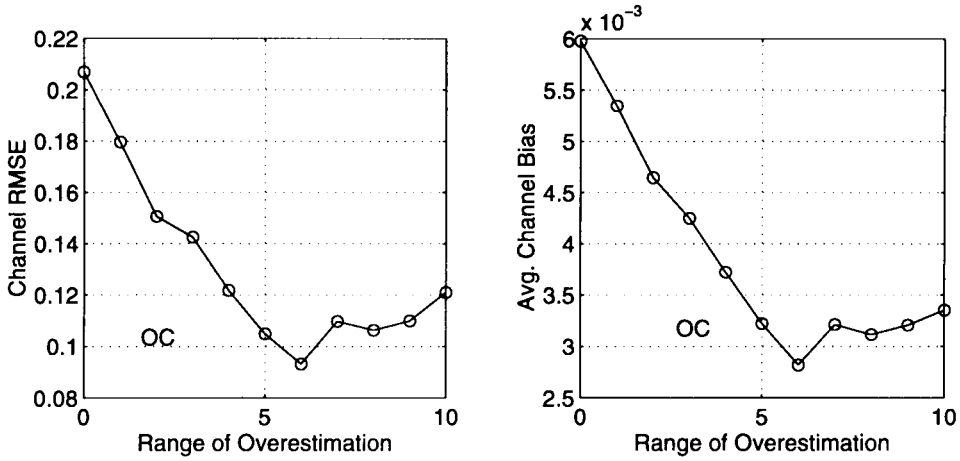

Fig. 10. Channel error versus overestimated order for $M = 15$, $I = 100$, 120 M data (with $P = M + L_h$ varying accordingly).

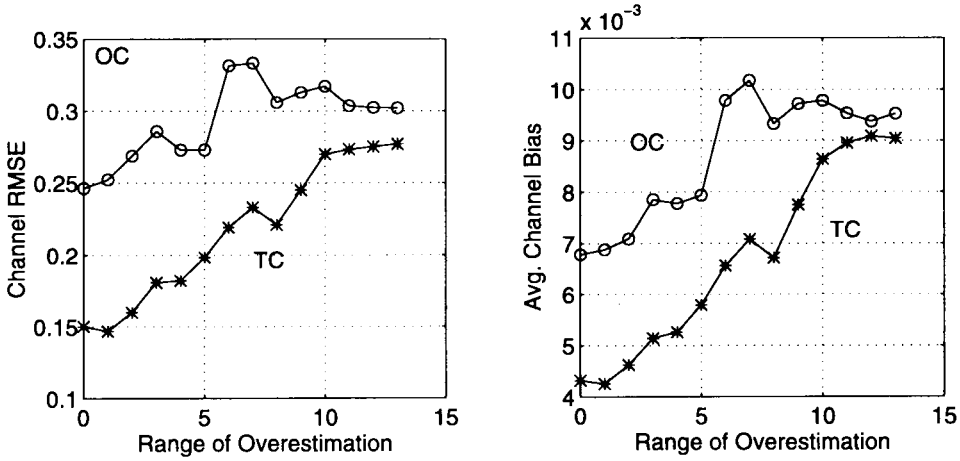

Fig. 11. Channel error versus overestimated order for $M = 15$, $P = 19$, $I = 100\,120$ M data.

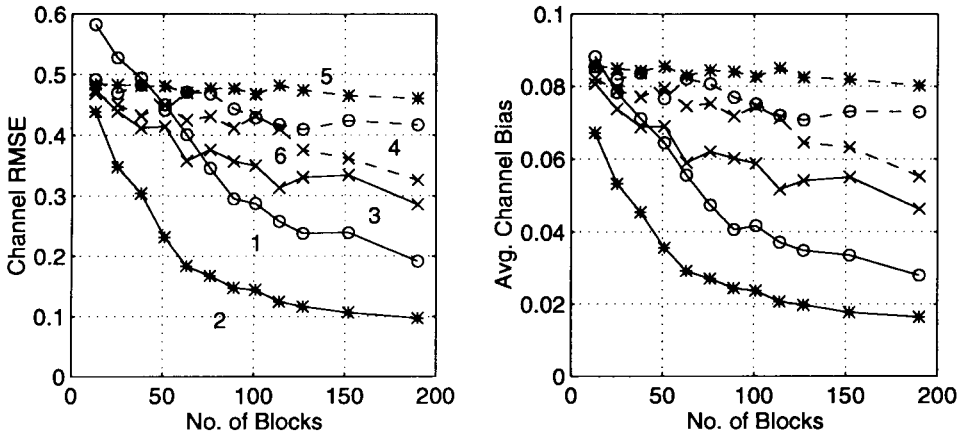

Fig. 12. Channel error versus number of blocks of data for $M = 15$, $P = 19$, $I = 100$ for the one cycle approach with cycles $1 \ldots 6$.

because of the orthogonality of the exponentials, and periodicity is lost. Linear, time-invariant filtering does not change cyclostationarity; consequently, we expect periodicity in the time-varying correlation at the output of the channel

$$c_{xx}(nP+p;\tau) = \sum_{l=0}^{L_h} h(l)h^*(l+\tau-q)c_{ww}(n-l;q) + c_{vv}(nP+p;\tau) \quad (7)$$

which is indeed the case. If the noise is AWGN, then it has a time-varying correlation that simplifies to $c_{vv}(nP + q;\tau) = \sigma_v^2\delta(\tau)$ in (7). To avoid stationary noise, we consider the cyclic correlation, which is defined as the Fourier series expansion of the time-varying correlation $C_{yy}(k;\tau) = (1/P)\sum_{p=0}^{P-1} c_{yy}(p;\tau)\exp(-j2\pi kp/P)$. The cyclic correlation of the encoder output is $C_{ww}(k;\tau) = (\sigma_s^2 M/P)\{\delta(\tau)\delta(k) + [\delta(\tau+M)\exp(-j2\pi kM/P) + \delta(\tau-M)]E(k)\}$ with $E(k) :=$

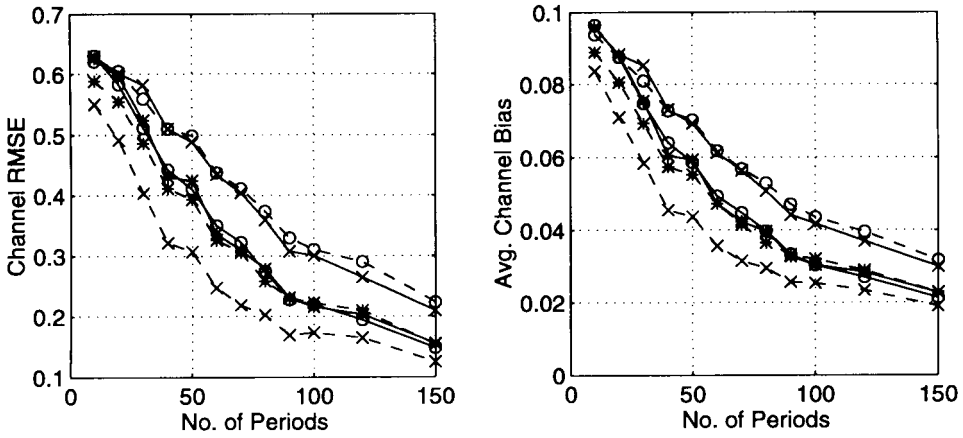

Fig. 13. Channel error versus number of blocks of data for $M = 15$, $P = 19$, $I = 100$ for the two cycle approach with cycle 1 and cycles $2, \ldots, 7$. Cycles are ordered $4, 3, 5, 1, 2, 6$ from top to bottom at 120 M.

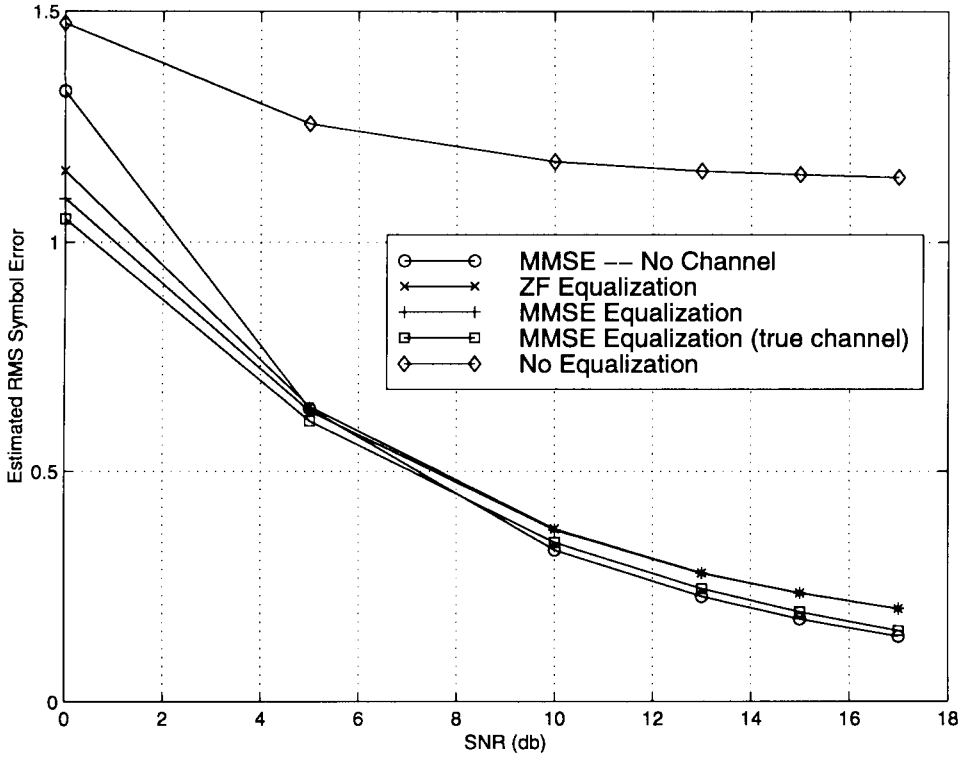

Fig. 14. RMS symbol estimation error—Adequate length cyclic prefix.

$\exp(-j\pi k(L-1)/P)\sin(\pi kL/P)/\sin(\pi k/P)$. We write the cyclic correlation of the channel output in (7) as

$$C_{xx}(k;\tau) = \sum_{l=0}^{L_h}\sum_{q=-M}^{M} h(l)h^*(l+\tau-q)C_{ww}(k;q)e^{-j\frac{2\pi}{P}kl} + C_{vv}(k;\tau). \tag{8}$$

The cyclic correlation of the noise is $C_{vv}(k;\tau) = \sigma_v^2\delta(\tau)\delta(k)$, which is zero for nonzero cycles k. Subsequently, we will assume that $k \neq 0$ to avoid stationary noise.

The Z transform of the cyclic correlation with respect to τ defines the cyclic spectrum. For a particular cycle $k \neq 0$, the output cyclic spectrum is $S_{xx}(k;z) = S_{ww}(k;z)$ $H(\exp(-j2\pi k/P)z^{-1})H^*(z^*)$, where $S_{ww}(k;z) = \sigma_s^2(M/P)$ $\{\delta(k) + [z^{-M}\exp(-j2\pi kM/P) + z^M]E(k)\}$. Interestingly, if we examine two cycles k_1 and k_2, we can take the ratio of the cyclic spectra to find

$$S_{xx}(k_1;z)S_{ww}(k_2;z)H\left(e^{j\frac{2\pi}{P}k_2}z^{-1}\right) = S_{xx}(k_2;z)S_{ww}(k_1;z)H\left(e^{j\frac{2\pi}{P}k_1}z^{-1}\right). \tag{9}$$

In the following development, we will only consider admissible cycles k, as defined in the following proposition.

Proposition 1: A cycle k is admissible if $k \neq 0$, and $C_{ww}(k;\tau)$ is nonzero for at least one lag τ. This occurs if k is chosen such that $kL \bmod P \neq 0$. The set of all admissible cycles is nonempty, e.g., choose L even and P odd.

Proof: If $kL \bmod P \neq 0$, it follows that $\sin(\pi kL/P) \neq 0$, which for $k \neq 0$ implies that $E(k) \neq 0$, and hence, $C_{ww}(k;\tau) \neq 0$ for at least one τ, namely, $\tau = M$ or $\tau = -M$. □

To solve for the channel, we write (9) in matrix form. With $'$ as transpose, let $\mathbf{h} = [h(0)\cdots h(L_h)]'$ and $\mathbf{D}_k(L_h) =$

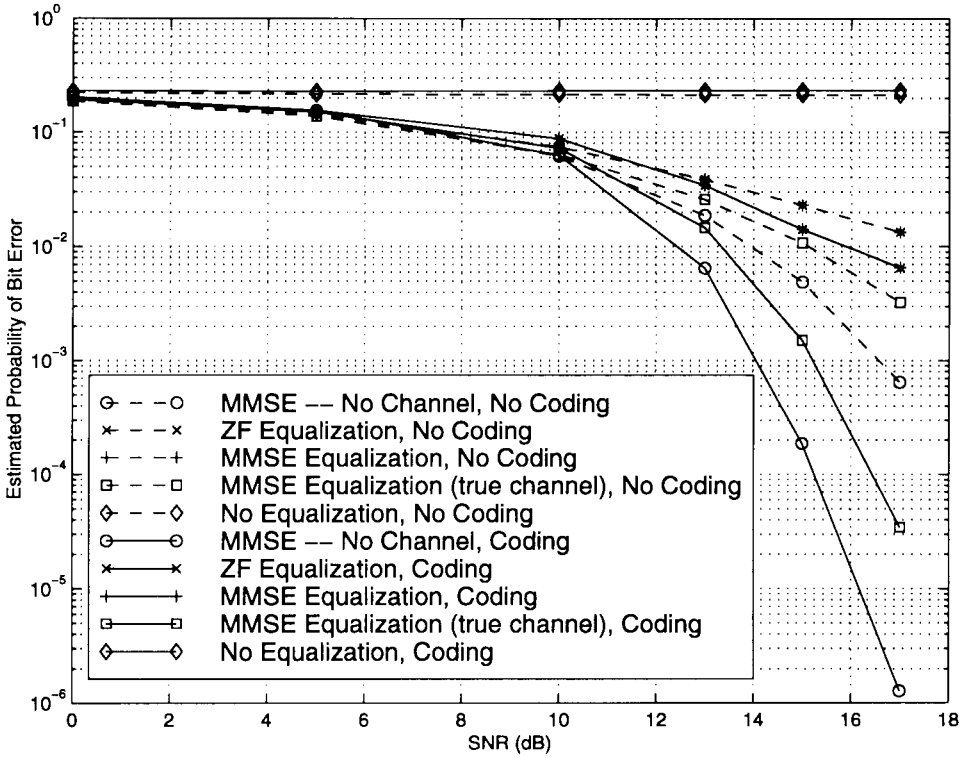

Fig. 15. Estimated probability of bit error with adequate-length cyclic prefix.

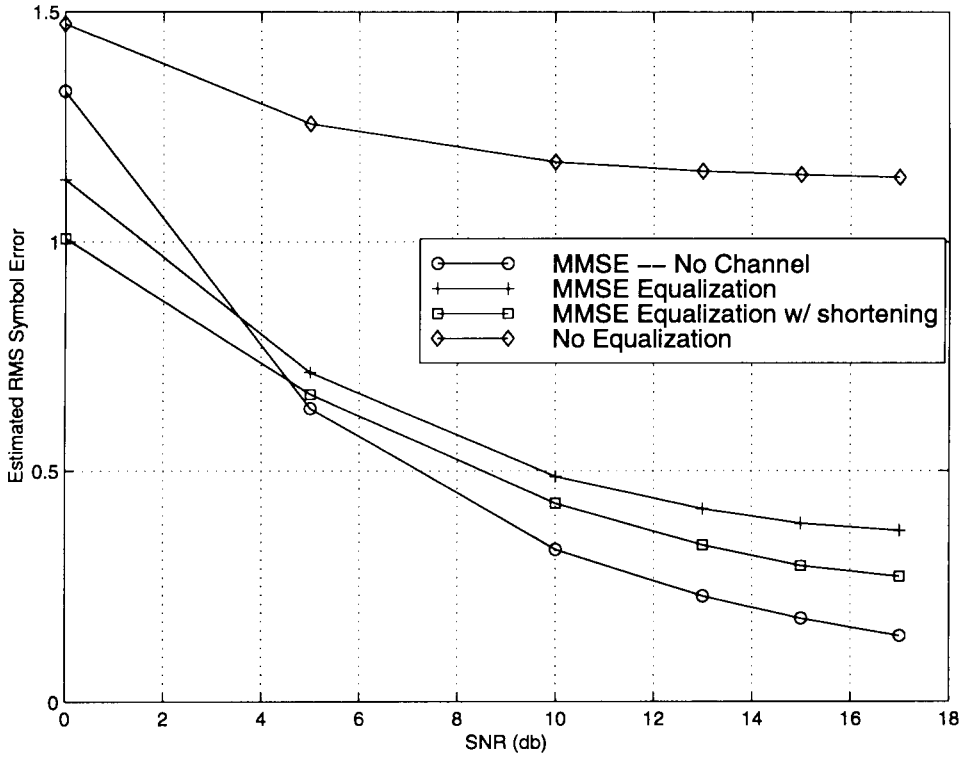

Fig. 16. RMS symbol error—Inadequate length cyclic prefix.

diag$(1, \ldots, \exp(j2\pi k L_h/P))$. Then, let $\mathcal{T}_k^{(w)}$ denote the $(2M + L_h + 2) \times (L_h + 1)$ Toeplitz matrix with first column $[C_{ww}(k;-M), \ldots, C_{ww}(k;M), 0, \ldots, 0]$ and first row $[C_{ww}(k;-M), 0, \ldots, 0]$. Similarly, let $\mathcal{T}_k^{(x)}$ denote the $(4M + 2L + L_h + 3) \times (2M + L_h + 2)$ matrix with first column $[C_{xx}(k;-M - L_h), \ldots, C_{xx}(k;M + L_h), 0, \ldots, 0]$ and first row $[C_{xx}(k;-M - L_h), 0, \ldots, 0]$. Then, we rewrite (9) and can solve for the channel (within a scale nonidentifiable blindly) from

$$\mathcal{T}\mathbf{h} = \mathbf{0}, \quad \mathcal{T} := \left[\mathcal{T}_{k_2}^{(x)}\mathcal{T}_{k_1}^{(w)}\mathbf{D}_{k_1} - \mathcal{T}_{k_1}^{(x)}\mathcal{T}_{k_2}^{(w)}\mathbf{D}_{k_2}\right]. \tag{10}$$

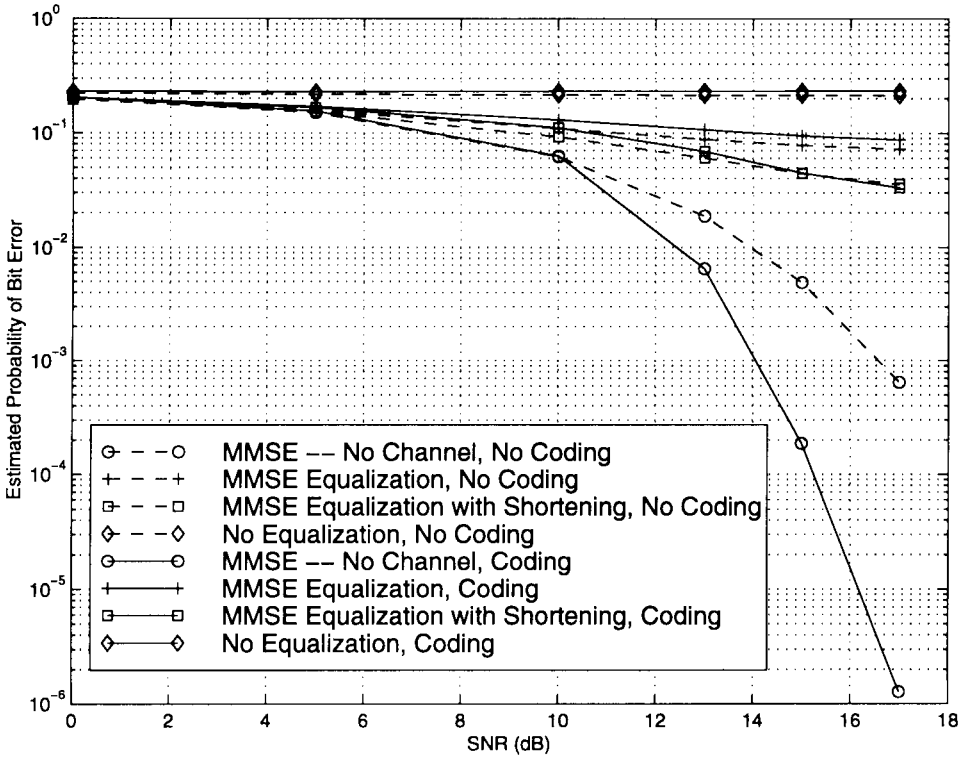

Fig. 17. Estimated probability of bit error with inadequate-length cyclic prefix.

Note that $\mathbf{D}_k$ and $\mathcal{T}_{k_i}^{(w)}$ are known *a priori* while the coefficients of $\mathcal{T}_k^{(x)}$ are the cyclic correlations at the receiver, which can be consistently estimated using the sample cyclic correlation estimator $\hat{C}_{xx}(k;\tau) = (1/N)\sum_{n=0}^{N-1} x(n)x^*(n+\tau)\exp(-j2\pi kn/P)$. Identifiability of the channel from (10) is established in the following proposition.

Proposition 2: The channel $\{h(l)\}_{l=0}^{L_h}$ is uniquely identifiable within a complex scalar from (10) if and only if k_1 and k_2 are both admissible, and there is no $l \in [1, L_h]$ such that $\exp(-j2\pi k_1 l/P) = \exp(-j2\pi k_2 l/P)$.

Proof: The proof follows from the proof in [13] by noting that the product $\mathcal{T}_{k_i}^{(x)}\mathcal{T}_{k_j}^{(w)}$ is a product of Toeplitz matrices, which is Toeplitz. □

One interesting pair of cycles is k and $-k$. Because $C_{xx}(-k;\tau) = C_{xx}^*(k;-\tau)\exp(-j2\pi k\tau/P)$ in $S_{xx}(k;z)$ and $S_{xx}(-k;z)$, we can solve for the channel from (10) using only one cyclic correlation, which we call the one-cycle (OC) approach. Alternatively, with two cycles, we can use a two-cycle (TC) approach and build three sets of equations like (10) to possibly increase estimation accuracy. Note that with slight modification, this channel identification formulation can be applied to any transmitter that has a cyclostationary outputs.

Given a set of admissible cycles, it is desirable to know which two cycles k_1 and k_2 to choose to find the channel. From the cyclic spectrum, we would like to pick the cycles such that $S_{ww}(k_1;z)$ and $S_{ww}(k_2;z)$ are the "most different:" a requirement that is difficult to quantify. Since $S_{ww}(k_i;z)$ is only a function of $C_{ww}(k_i;M)$ and $C_{ww}(k_i;-M)$, one option is to pick k_i such that $|C_{ww}(k_i;M)|$ (which conveniently equals $|C_{ww}(k_i;-M)|$) is maximum. From the expression for $C_{ww}(k_i;M)$ (8), this occurs when k_i is chosen such that $|E(k)|$ is maximized. Due to the odd symmetry of the sine function, for any k that maximizes $|E(k)|$, $-k$ will also maximize $|E(k)|$, and such a choice of k and $-k$ results in the OC solution of (10). If we wish to use the TC solution, we should pick the cycles k_1 and k_2, which maximizes $|E(k)|$ subject to the constraint that $|k_2| \neq |k_1|$. With this choice of cycles, we will be estimating the cyclic correlations that have the most significant energy when compared with the noise power and using these coefficients to find the channel. We use this method of cycle selection in the simulations that follow.

IV. Simulations

In this section, we examine the performance of the OC, TC channel estimates in the OFDM system. We use the root mean square error (RMSE), which is defined as $\frac{1}{\|\mathbf{h}\|}\sqrt{\frac{1}{I(L_h+1)}\sum_{i=0}^{I}\|\hat{\mathbf{h}}^i - \mathbf{h}\|^2}$, and the channel average bias $\frac{1}{I(L_h+1)}\sum_{l=0}^{L_h}|\sum_{i=0}^{I}\hat{h}^i(l) - h(l)|$, both averaged over I Monte Carlos to evaluate the channel error. To evaluate the usefulness of the channel estimator in the receiver, we employ the symbol RMSE $\frac{1}{\sigma_s^2}\sqrt{\frac{1}{IN}\sum_{i=0}^{I}\sum_{j=0}^{N}|\hat{s}^i(l) - s(l)|^2}$ and the estimated probability of bit error.

Experiment 1: Here, we consider a two-ray multipath channel $h_c(t) = e^{-j2\pi(0.15)}r_c(t - T/2, \beta) + 0.8\, e^{-j2\pi(0.6)}r_c(t - 5T/4, \beta)$, where $r_c(t)$ is the raised cosine[1] with rolloff $\beta = 0.35$ sampled at $t = 0, T, \ldots, 4T$; thus, $L_h = 4$. We used $I = 100$, $M = 15$, and $16-$QAM for modulation. In Fig. 6, with $P = 19$, we show the average channel estimate for SNR = 20 dB and 120 M data along with the channel error versus the number of blocks in Fig. 7. The corresponding performance for 120 M data varied over SNR is displayed in Fig. 8. From Figs. 7 and 8, we see that the estimator is consistent and that the estimates improve as the noise power decreases. In Fig. 9, for SNR = 20 dB and 120 M symbols, we consider the channel error as $P = M + L$ and varies from $L = 1, \ldots, 15$, whereas the channel is fixed to observe how the estimate depends on the difference $L = P - M$. From Fig. 9, we see that although the estimator works with L as small as 1, increasing the length of the cyclic prefix decreases the error. This is intuitively appealing because

[1] See [10] for information about the use of the raised-cosine pulse-shapping filter in OFDM.

we would like to trade off extra redundancy for error performance. Next, we consider the channel RMSE for SNR = 20 dB when the order L_h is overestimated and $P = M + L_h$ in Fig. 10 and when the order is overestimated with $P = 19$ in Fig. 11. In Fig. 10, we see the beneficial effects of having a larger prefix, whereas Fig. 11 shows the graceful degradation when the channel is overestimated.

Experiment 2: In this experiment, we consider the effect of the cycle chosen on the resulting channel error in estimating the two-ray channel above. Fig. 12 considers the performance of the OC approach for $I = 100$, $P = 19$, $M = 15$, SNR = 20 dB, and 120 M symbols for cycles 1 ... 6, whereas Fig. 13 considers similarly the performance using the TC approach with cycles 1 and 2 ... 7. Cycle selection seems to have an effect on the channel error, but asymptotic performance analysis is required to determine its precise role.

Experiment 3: Now, we look at the probability of bit error for an OFDM system. In Fig. 14, we plot the RMS symbol estimation error, and in Fig. 15, we plot the probability of bit error (assuming Gray coding in selection of the 16 QAM symbols) estimated over 500 Monte Carlos of 500 M data for an OFDM system with $M = 15$ and $P = 19$, with and without a $(15, 11)$ two symbol-error correcting Reed–Solomon (RS) equivalent code for the artificial channel $h = [1, 2, 1, -1, 1]/\sqrt{8}$. We used the standard OFDM ZF and MMSE structures [12] to equalize the $L_h = 4$ channel above. Next, we consider the same channel and $M = 15$ and $P = 17$ to observe the effects of channels longer than the cyclic prefix. We estimate the channel as before but look at MMSE equalization with and without the use of impulse response shortening [9] and RS$(15, 11)$ coding. We used an eight-tap, zero-delay shortening filter derived from the estimated channel. In Fig. 16, we plot the RMS symbol estimation error, and in Fig. 17, we plot the estimated probability of error. For comparison purposes, in Figs. 15 and 17, we plot the MMSE uncoded and coded solutions for the case when $h(n) = \delta(n)$ as well as when there is no attempt at equalization. In Fig. 15, we see that the performance of the system using equalization with our channel estimate approaches the performance of the case where $h(n) = \delta(n)$. From Fig. 17, we see that impulse response shortening may be a beneficial technique when combined with our channel estimate since it reduces the the error floor present in the unshortened scenario. Performance of impulse response shortening varies with the channel and may be improved by changing shortening parameters. Further improvements may be obtained using vector MMSE or vector MMSE decision feedback equalizers at the expense of further complexity [6].

REFERENCES

[1] P. S. Chow, J. M. Cioffi, and J. A. C. Bingham, "A practical discrete multitone transceiver loading algorithm for data transmission over spectrally shaped channels," *IEEE Trans. Commun.*, vol. 43, pp. 773–775, Mar. 1995.

[2] L. J. Cimini, Jr., "Performance studies for high-speed indoor wireless communications," *Wireless Pers. Commun.*, vol. 2, nos. 1–2, pp. 67–85, 1995.

[3] M. de Courville, P. Duhamel, P. Madec, and J. Palicot, "A least mean squares blind equalization techniques for OFDM systems," *Ann. Telecommun.*, vol. 52, nos. 1–2, pp. 12–20, Jan.–Feb. 1997.

[4] Z. Ding, "Characteristics of band-limited channels unidentifiable from second-order cyclostationary statistics," *IEEE Signal Processing Lett.*, vol. 3, pp. 150–152, May 1996.

[5] G. B. Giannakis, "Filterbanks for blind channel identification and equalization," *IEEE Signal Processing Lett.*, vol. 4, pp. 184–187, June 1997.

[6] R. W. Heath, Jr., "Mitigating channel distortions in wireless orthogonal frequency division multiplexing communication systems," Dept. Elect. Eng., Univ. Virginia, Charlottesville, Aug. 1997.

[7] J. W. Lechleider, "The optimum combination of block codes and receivers for arbitrary channels," *IEEE Trans. Commun.*, vol. 38, pp. 615–621, May 1990.

[8] B. L. Floch, M. Alard, and C. Berrou, "Coded orthogonal frequency division multiplex," *Proc. IEEE*, vol. 83, pp. 982–996, June 1995.

[9] P. Melsa, R. C. Younce, and C. E. Rohrs, "Impulse response shortening for discrete multitone transceivers," *IEEE Trans. Commun.*, vol. 44, pp. 1662–1672, Dec. 1996.

[10] T. Pollet and M. Moeneclaey, "The effect of carrier frequency offset on the performance of band limited single carrier and OFDM signals," in *Proc. GLOBECOM*, London, U.K., Nov. 18–22, 1996, pp. 719–723.

[11] H. Sari, G. Karam, and I. Jeanclaude, "An analysis of orthogonal frequency-division multiplexing for mobile radio applications," in *Prof. Vehic. Technol. Conf.*, Stockholm, Sweden, June 8–10, 1994, pp. 1635–1639.

[12] H. Sari, G. Karam, and I. Jeanclaude, "Transmission techniques for digital terrestrial TV broadcasting," *IEEE Commun. Mag.*, pp. 100–109, Feb. 1995.

[13] E. Serpedin and G. B. Giannakis, "Blind channel identification and equalization using modulation induced cyclostationarity," *IEEE Trans. Signal Processing*, vol. 46, pp. 3099–3104, Nov. 1998; see also *Proc. 31st Conf. Inform. Sci. Syst.*, Johns Hopkins Univ., Baltimore, MD, vol. II, Mar. 19–21, 1997, pp. 792–797.

[14] M. K. Tsatsanis and G. B. Giannakis, "Transmitter induced cyclostationarity for blind channel equalization," *IEEE Trans. Signal Processing*, vol. 45, pp. 1785–1794, July 1997.

[15] J.-J. van de Beek, M. Sandell, and P. O. Börjesson, "ML estimation of time and frequency offset in OFDM systems," *IEEE Trans. Signal Processing*, vol. 45, pp. 180–1805, July 1997.

[16] L. Vandendorpe, "MMSE equalizers for multitone systems without guard time," in *Proc. Euro. Signal Process. Conf.*, Sept. 10–13, 1996.

[17] E. Viterbo and K. Fazel, "How to combat long echoes in OFDM transmission schemes: Sub-channel equalization or more powerful channel coding," in *Proc. GLOBECOM*, Singapore, Nov. 14–16, 1995, pp. 2069–2074.

On the Equivalence of Blind Equalizers Based on MRE and Subspace Intersections

David Gesbert, Alle-Jan van der Veen, and A. Paulraj

***Abstract*—Two classes of algorithms for multichannel blind equalization are the mutually referenced equalizer (MRE) method by Gesbert *et al.*, and the subspace intersection (SSI) method by van der Veen *et al.* Although these methods seem, at first sight, unrelated, we show here that certain variants of the SSI and the MRE methods both optimize a new blind criterion, which is referred to as *maximum coherence* and, thus, are equivalent.**

***Index Terms*—Array signal processing, fractionally spaced equalization, mobile communications, multichannel blind equalization.**

I. INTRODUCTION

Blind equalization has been an active research area during the last few years. Two major factors appear to drive the wide interest in this topic. First, there is an increasing number of interesting and promising applications in the area of digital communications: wireless

Manuscript received February 17, 1998; revised August 4, 1998. The associate editor coordinating the review of this paper and approving it for publication was Dr. Lai C. Godara.

D. Gesbert and A. Paulraj are with the Information Systems Laboratory, Stanford University, Stanford CA 94305 USA (e-mail: gesbert@rascals.stanford.edu).

A.-J. van der Veen is with the Department of Electrical Engineering/DIMES, Delft University of Technology, Delft, The Netherlands.

Publisher Item Identifier S 1053-587X(99)01349-5.